Figure S1. Age distribution of BSGS subjects with DNA methylation data.
DNA methylation data was measured in 610 individuals from the Brisbane System Genetics Study. The ages of the individuals range from 10 to 75 years, with a mean age of 21 years.

Type I Error Rate and Power

To estimate the type I error rate and our power to detect age-dependent changes in genetic and environmental variance, we performed simulations under the null and alternative hypotheses. We first estimated type I error by simulating residualized β-values at 10,000 CpG sites under the null hypothesis, where the genetic and environmental variance are independent of age, or γ_g and γ_e are equal to zero. For each CpG site a residualized β-value, $X_{it_{sim}}$, was simulated for each individual i at age t

$$X_{it_{sim}} = \alpha + \beta_{age}t + \beta_{sex}male + G_i + E_i \qquad (S1)$$

where G_i and E_i are generated random variables representing genetic and environmental contributions respectively. The environmental contributions E_i were generated from a normal distribution with mean zero and variance equal to the environmental variance estimated from the BSGS data. The genetic contributions G_i were generated from a multivariate normal distribution with mean zero and variance equal to $2\phi_{ij}\sigma_g^2$, where ϕ_{ij} is the kinship coefficient matrix from the BSGS subjects and σ_g^2 is the genetic variance estimated from the BSGS data. This formulation allows our generated genetic residuals to be correlated between relatives as in the original data. For each CpG site, the remaining coefficients in this model, α, β_{age}, and β_{sex}, take on values estimated from the BSGS data using equation (1).

At each CpG site, the generated vector $X_{it_{sim}}$ was used as the phenotype to estimate γ_g and γ_e via equation (2). At a significance level of $\alpha = 0.05$, 5.94% of the CpG sites had a γ_g

significantly different from 0, and 5.82% of CpG sites had a γ_e significantly different from 0 (Table S1). Figure S2 compares the distributions of γ_g and γ_e P-values, and shows nearly identical distributions at all reasonable levels of significance. These results suggest that our modeling approach has appropriate levels of type I error.
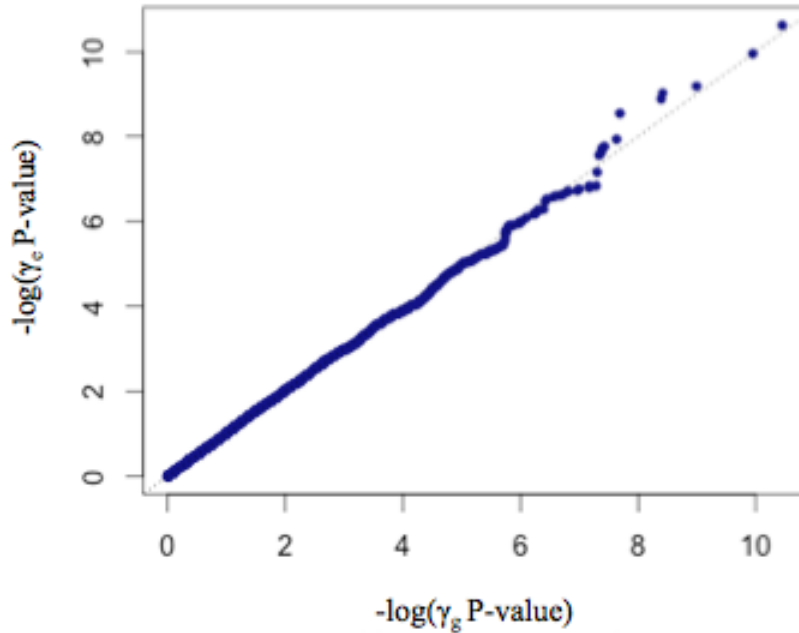
Figure S2. A quantile-quantile (Q-Q) plot for type I error simulations of γ_g and γ_e. This plot compares the distribution of γ_g p-values to the distribution of γ_e p-values. Identical distributions will lie along the identity line, shown here as a dashed line.

To estimate power we simulated normalized β-values at 10,000 CpG sites under the alternative hypothesis that the genetic and environmental variances are age-dependent, and γ_g and γ_e are non-zero. To generate these effects, we modified G_i and E_i in equation (S1) to include age-dependent terms according to the model in equation (2). The scale of the age dependence for our simulations was set to the mean of the absolute values of γ_g and γ_e estimated from the BSGS data, such that it took the same value for simulation of both G_i and E_i.

The modified G_i and E_i with age-dependent effects were used to generate new vectors of $X_{it_{sim}}$ as defined in equation (S1). As before, the generated vector $X_{it_{sim}}$ was used as the phenotype to calculate γ_g and γ_e via equation (2) for each CpG site. At a significance level of α = 0.05, 44.9% of the CpG sites had a γ_g that was significantly different from 0, and 51.2% of the CpG sites had a γ_e that was significantly different from 0 (Table S1). Figure S3 compares the distributions of γ_g and γ_e P-values, and shows nearly identical distributions at reasonable levels of significance. This confirms that we have approximately equivalent power to detect age-dependent changes in the genetic and environmental variances with γ_g and γ_e.
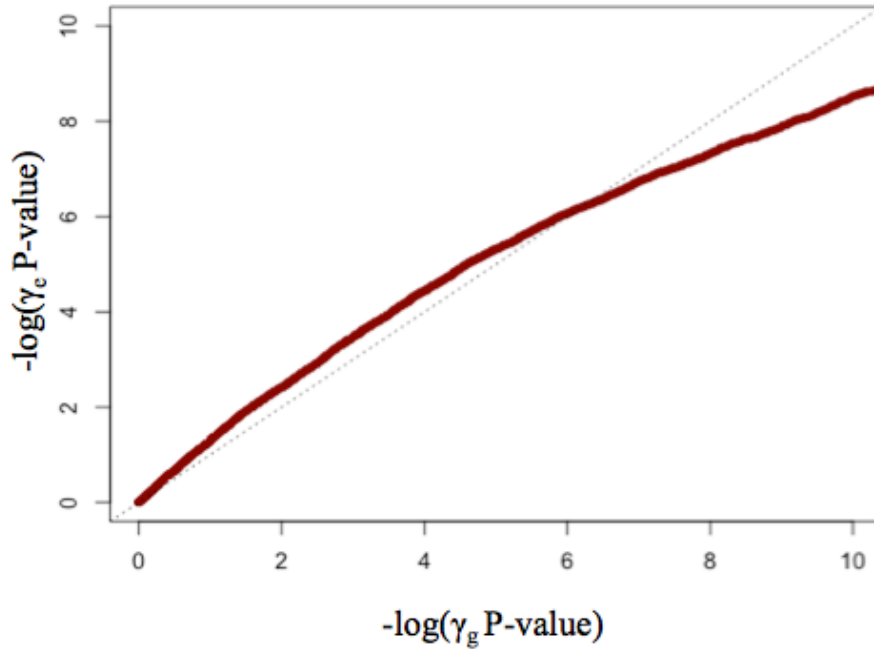
Figure S3. A quantile-quantile (Q-Q) plot for power simulations of γ_g and γ_e. This plot compares the distribution of γ_g p-values to the distribution of γ_e p-values. Identical distributions will lie along the identity line, shown here as a dashed line.

Table S1. Type I error rate and power for age-dependent changes in genetic and environmental variance.

	TYPE I ERROR $\gamma_g = 0, \gamma_e = 0$	POWER $\gamma_g \neq 0, \gamma_e \neq 0$
Proportion of significant γ_g	0.0594	0.4492
Proportion of significant γ_e	0.0582	0.5119

The age-dependence of genetic variance is reflected by γ_g.
The age-dependence of environmental variance is reflected by γ_e.
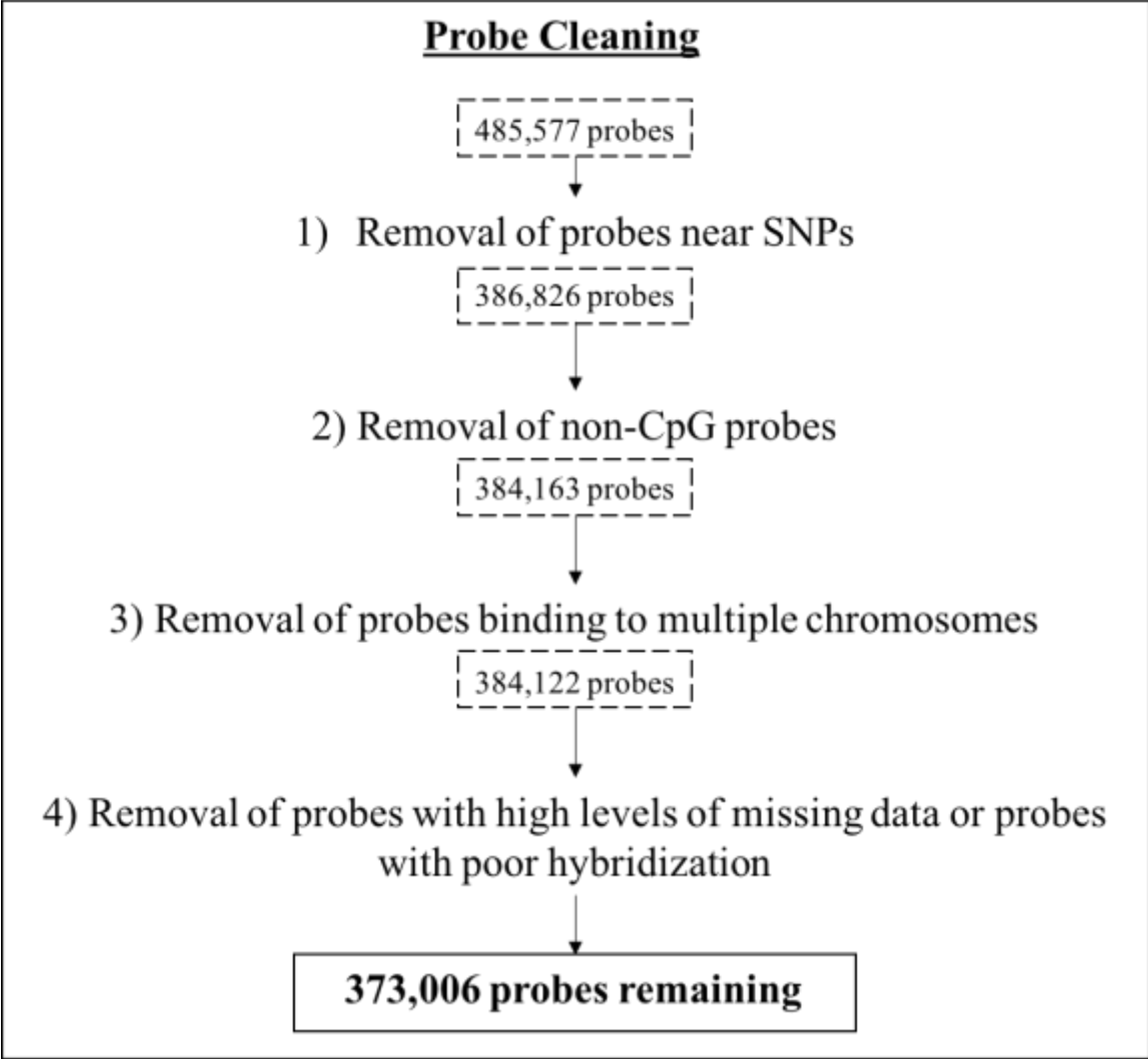
Figure S4. Data cleaning process for BSGS DNA methylation data.
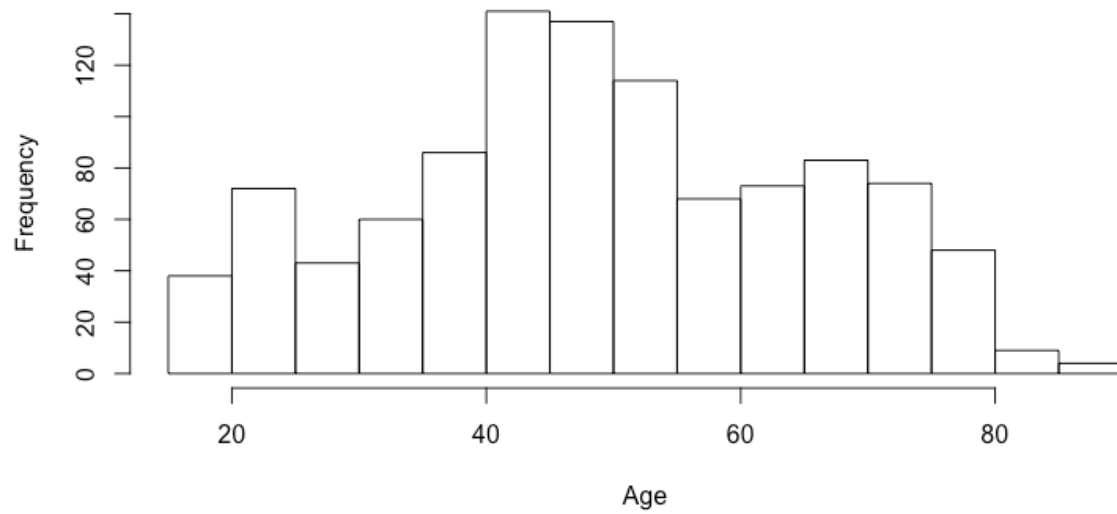
Figure S5. Age distribution of GOLDN subjects with DNA methylation data.
DNA methylation data was measured in 1050 individuals from the GOLDN Study. The ages of the individuals range from 18 to 88 years, with a mean age of 49 years.
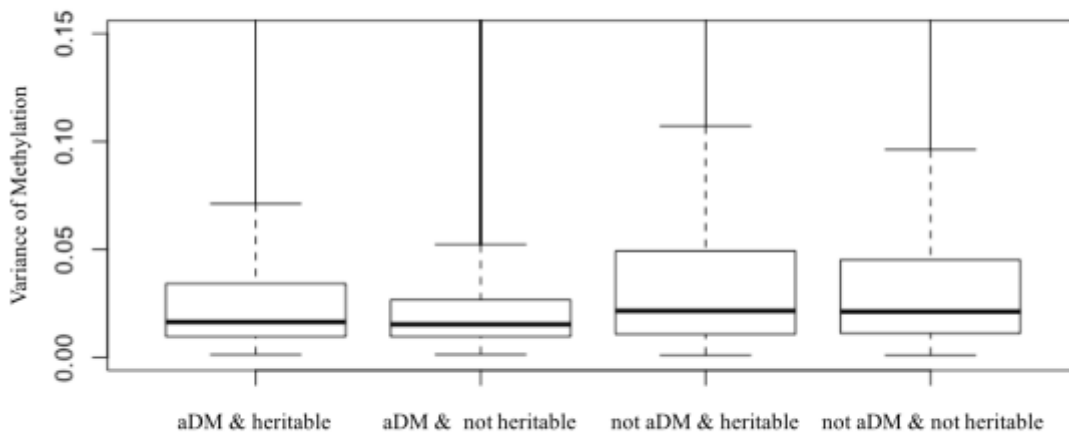
Figure S6. Boxplots comparing the distribution of methylation variance at CpG sites categorized by aDM and heritability status.

Table S2. Gene Ontology Terms. Total counts and the significant terms for MA and DS after multiple test correction (FDR<0.05).

ONTOLOGY	MA		DS	
	COUNT		COUNT	
	TERM | ADJUSTED P-VALUE		TERM | ADJUSTED P-VALUE	
MOLECULAR FUNCTION	**3**		**2**	
	Sequence-specific DNA binding	5.88E-7	Sequence-specific DNA binding	2.23E-8
	Double-stranded DNA binding	9.90E-4	Double-stranded DNA binding	2.39E-2
	Transcriptional activator activity, RNA polymerase II core promoter proximal region sequence-specific binding	9.98E-3		
CELLULAR COMPONENT	**2**		**0**	
	Integral component of plasma membrane	2.07E-4		
	Cell junction	1.80E-2		
BIOLOGICAL PROCESSES	**19**		**5**	
	Positive regulation of nucleobase-containing compound metabolic process	4.52E-5	Positive regulation of nucleobase-containing compound metabolic process	9.07E-4
	Cardiovascular system development	4.52E-5	Positive regulation of transcription from RNA polymerase II promoter	9.07E-4
	Positive regulation of RNA biosynthetic process	8.44E-5	Negative regulation of transcription from RNA polymerase II promoter	9.07E-4
	Sensory organ morphogenesis	2.04E-3	Positive regulation of RNA biosynthetic process	6.01E-3
	Multicellular organism development	2.04E-3	Pattern specification process	6.01E-3
	Tissue development	3.24E-3		
	Positive regulation of transcription from RNA polymerase II promoter	3.57E-3		
	Inner ear morphogenesis	1.13E-2		
	Embryo development ending in birth or egg hatching	1.13E-2		
	Localization	1.22E-2		
	Negative regulation of transcription from RNA polymerase II promoter	1.56E-2		
	Negative regulation of multicellular organismal process	1.56E-2		
	Embryonic forelimb morphogenesis	1.64E-2		

	Morphogenesis of a branching structure	1.84E-2			
	Positive regulation of neuron differentiation	3.34E-2			
	Regulation of cellular component movement	4.37E-2			
ALL	**24**			**7**	

Table S3. Expression analysis of replicated MA sites with significant γ_g. Significant expression and methylation associations after multiple test correction (FDR < 0.05).

CPG SITE LOCATION	ASSOCIATED EXPRESSION PROBE	DIRECTION OF ASSOCIATION	P-VALUE	GENE	LOCATION OF TSS
cg02914422 Chr 7: 32110145	ILMN_1778788	Negative	1.03×10^{-5}	AMOTL2	Chr 3: 134094259
	ILMN_3272768	Negative	4.63×10^{-6}	LINC00339	Chr 1: 22351683
	ILMN_2397199	Negative	9.67×10^{-6}	NDEL1	Chr 17: 8339169
	ILMN_1786734	Negative	1.06×10^{-5}	EIF5	Chr 14: 103800338
cg05691152 Chr 22: 38092978	ILMN_1684585	Negative	6.07×10^{-6}	ACSL1	Chr 4: 185747268
	ILMN_1694548	Negative	$8,40 \times 10^{-6}$	ANXA3	Chr 4: 79472741
	ILMN_1715068	Negative	1.13×10^{-5}	AQP9	Chr 15: 58430407
	ILMN_1694243	Negative	1.53×10^{-6}	LILRA6	Chr 19: 54746617
	ILMN_1714643	Negative	$4,87 \times 10^{-6}$	MGAM	Ch 7: 141695678
	ILMN_2114720	Negative	2.90×10^{-6}	SLPI	Chr 20: 43880879
cg13672736 Chr 9: 136114066	ILMN_1678535	Positive	7.37×10^{-6}	ESR1	Chr 6: 152011630